JGR Biogeosciences

RESEARCH ARTICLE
10.1029/2020JG005724

Key Points:

- Soil (CO_2) doubled in the fall, likely attributable to complex changes in biological activity, storage, and transport processes amidst soil freezing
- Soil (CO_2) was significantly controlled by soil temperature and maintained substantial values well below zero (at −20 cm soil (CO_2) concentrations were in the order of 6.40 ± 0.19% through freezing)
- Peak increases in soil (CO_2) were not captured by ecosystem scale CO_2 fluxes, suggesting a disconnect between complex and spatially heterogenous driving processes

Supporting Information:

Supporting Information may be found in the online version of this article.

Correspondence to:

E. Wilkman,
ewilkman-w@sdsu.edu

Citation:

Wilkman, E., Zona, D., Arndt, K., Gioli, B., Nakamoto, K., Lipson, D. A., & Oechel, W. C. (2021). Ecosystem scale implication of soil CO_2 concentration dynamics during soil freezing in Alaskan Arctic tundra ecosystems. *Journal of Geophysical Research: Biogeosciences*, *126*, e2020JG005724. https://doi.org/10.1029/2020JG005724

Received 9 MAR 2020
Accepted 23 NOV 2020

Ecosystem Scale Implication of Soil CO_2 Concentration Dynamics During Soil Freezing in Alaskan Arctic Tundra Ecosystems

Eric Wilkman[1], Donatella Zona[1,2], Kyle Arndt[1,3], Beniamino Gioli[4], Kyoko Nakamoto[1], David A. Lipson[1], and Walter C. Oechel[1,5]

[1]Department of Biology, San Diego State University, San Diego, CA, USA, [2]Department of Animal and Plant Sciences, University of Sheffield, Sheffield, UK, [3]Earth Systems Research Center, Institute for the Study of Earth, Oceans, and Space, University of New Hampshire, Durham, NH, USA, [4]Consiglio Nazionale delle Ricerche, Institute for Bioeconomy, Florence, Italy, [5]Department of Geography, University of Exeter, Exeter, UK

Abstract The rates, processes, and controls on Arctic cold period soil carbon loss are still poorly understood. To understand one component of winter CO_2 loss in the atmosphere, continuous measurements of soil (CO_2) were made and compared to ecosystem scale CO_2 fluxes. Measurements of soil (CO_2) were made near Utqiaġvik, Alaska from the beginning of soil thaw in summer 2005 to spring 2007. In the summer, soil (CO_2) rose with increased soil temperature, reaching value orders of magnitude higher than the atmospheric (CO_2). Soil (CO_2) initially decreased at the end of summer and beginning of fall but then increased subsequent to soil freezing. Due to complex changes in biological activity, storage, and transport processes, soil (CO_2) was then approximately doubled than that was observed in the summer. After reaching peak concentrations in November, soil (CO_2) steeply decreased over a couple of weeks, suggesting a substantial release of CO_2 into the atmosphere and movement within the soil column. Eddy covariance (EC) measurements showed variable but continued emissions of CO_2 to the atmosphere during freezeup. The disconnect between soil (CO_2) and landscape level fluxes may be attributed to the spatiotemporal heterogeneity in release of high concentrations of soil (CO_2) to the atmosphere during the fall; and when integrated over the area of the EC tower footprint, do not frequently result in detectable emission events. Continued monitoring of fall and winter soil (CO_2) and ecosystem fluxes will be vital for further understanding the variability of interannual Arctic CO_2 emissions.

1. Introduction

1.1. Arctic Carbon Pools

The northern permafrost region underlies 15% of the global soil area, and the estimated organic carbon (C) pool in the upper 3 m in this region accounts for ~33% (1,035 ± 150 Pg C) of global belowground organic C storage (Hugelius et al., 2014; E. A. Schuur et al., 2015). It is reported that the high Arctic is becoming warmer and drier (Chapman & Walsh, 1993; Oechel et al., 1993, 1995, 2000; Polyakov et al., 2005); permafrost extent is shrinking and active layer thickness is increasing (Jorgenson et al., 2001; Serreze et al., 2002; Zhang et al., 2005). Historically, these northern ecosystems have acted as consistent C sinks, sequestering large stores of atmospheric C due to photosynthetic dominance in the short summer season and low rates of decomposition throughout the rest of the year as a consequence of cold, nutrient poor and generally water-logged conditions. However, currently much of this previously stored C is at risk of loss to the atmosphere due to accelerated soil organic matter decomposition in warmer future climates (Grogan & Chapin, 2000; Marion & Oechel, 1993; Nadelhoffer et al., 1992; Oechel et al., 1993). Increases in aerobic conditions, through lower water tables and higher soil temperature, increase the rates of soil respiration as soil becomes dry (Billings, 1983; Oechel et al., 1998). As such, the predicted warming and drying of the Arctic could release much of the C now stored in Arctic soils (E. A. G. Schuur et al., 2008). Significant CO_2 release has been observed from Greenland heath soils at the beginning of thaw, and the wet soil could trap large amounts of CO_2 during freezeup (Elberling & Brandt, 2003). Mastepanov et al. (2008, 2013) also reported that significant amounts of trapped methane (CH_4) escaped through fissures in frozen soils. Thus, phase changes between thawing and freezing could significantly affect gas transport. Nevertheless, the physical processes of gas transport in frozen soils have not been thoroughly examined to date, and the mechanisms responsible for this release are poorly understood and quantified, with relatively few studies extending into the fall and winter seasons (McGuire et al., 2012).

Warming is predicted to be greatest during winter, increasing by an estimated 4.8°C by 2100 as compared to 2.2°C during the summer months (Christensen et al., 2013). Nonetheless, winter C fluxes remain a key unknown in estimating the annual C balance of the tundra (Belshe et al., 2013; Björkman, Morgner, Björk et al., 2010; Euskirchen et al., 2012; McGuire et al., 2012). The fall and winter seasons are especially important as CO_2 losses can make up between 20% and 50% of an ecosystem's annual C loss, with estimates of winter CO_2 fluxes ranging from 0.19 to 210 g CO_2-C m^2 yr^{-1} (Björkman, Morgner, Cooper et al., 2010; Elberling & Brandt, 2003; Euskirchen et al., 2012; Fahnestock et al., 1999; Natali et al., 2019; Zimov et al., 1996). Winter C loss in the pan-Arctic is recently estimated at 1662 (±813) Tg C yr^{-1} with a predicted increase of 41% by the end of the century with accelerated warming (Natali et al., 2019). There is much uncertainty as to the bounds on these emissions, but nongrowing season C losses are thus seen as critical to the annual C balance, potentially shifting these ecosystems from sinks to sources over the next century (Commane et al., 2017; Euskirchen et al., 2017; Oechel et al., 2014; Treat et al., 2018; Zona et al., 2016).

1.2. Permafrost Processes

Arctic ecosystems are broadly characterized by permafrost, soils which are at or below the freezing point of water for two or more consecutive years (E. A. Schuur et al., 2015). Permafrost soils can be divided into three horizons based on temperature and depth: active, transient, and intermediate layers (Ping et al., 2015). The active layer, the uppermost soil horizon that thaws in the summer and freezes in the winter, is characterized by extreme temperature fluctuations that can vary between +15 and −35°C (Arctic Climate Impact Assessment, 2004). The transient permafrost sediments directly below are generally between 0.5 and 20 cm thick, have smaller temperature ranges, and may occasionally thaw during warm periods. The transient layer is itself underlain by the intermediate layer (Kanevskiy et al., 2017). During the fall shoulder season, rapid changes occur in the active layer that can amplify C losses from Arctic soils (Hinkel, 2001). At the outset of the fall freezeup period, the soil profile becomes isothermal at 0°C and gradually freezes bidirectionally from the top down and bottom up as ice forms adjacent to the permafrost floor and the soil surface. This soil freezing and thawing generates abrupt changes with sudden alterations in water content, changes in microbial metabolism, and increased nutrient mobilization (Elberling & Brandt, 2003; Henry, 2007; Kim et al., 2012; Yu et al., 2011). During freezeup, thermal contraction can also cause soil cracking, which modifies soil physical properties including diffusivity (Kerfoot, 1972; Pirk et al., 2016). Generally, freezing decreases substrate availability and substrate diffusivity including the diffusion of oxygen and CO_2. These fall seasonal changes can thus reduce rates of anaerobic metabolism and methanogenesis deep in the soil column (Rivkina et al., 2007; Yu et al., 2011). However, soil water can exist in the liquid state at temperatures significantly below the equilibrium freezing point of pure water (Panikov et al., 2006). The amount of liquid water that remains at subzero temperatures depends on localized capillary and surface absorption effects (Koopmans & Miller, 1966). Additionally, the partitioning of water between frozen and unfrozen states varies strongly with temperature, matric potential, and the osmotic potential of soil solution (Banin & Anderson, 1974; Drotz et al., 2009; Stähli & Stadler, 1997). In the Arctic, liquid water films have been seen to persist down to at least −10°C (Romanovsky & Osterkamp, 2000). In Utqiaġvik, Alaska, unfrozen volumetric water content through freezeup ranges from 0.18 to 0.02 cm^3/cm^{-3} at 20 cm depth, while active layer liquid saturation can remain at 5%–10% after freezeup (Hinkel et al., 2001; Mölders & Romanovsky, 2006). The presence of liquid water is vital for the continued activity of microbial communities, and as water films persist at bulk soil temperatures well below 0°C, microbial activity can be maintained at subzero temperatures (Coxson & Parkinson, 1987; Hinzman et al., 1991; Mikan et al., 2002; Panikov et al., 2006).

1.3. Nongrowing Season Dynamics

The importance of cold period CO_2 flux in the Arctic has been emphasized in the literature over the last few decades (Fahnestock et al., 1998; Jones et al., 1999; Kim et al., 2007; Oechel et al., 2000; Zimov et al., 1993). Nevertheless, given the harsh weather conditions, there are still relatively few continuous ecosystem scale measurements and sparse soil (CO_2) records available during the cold period in the Arctic (Kade et al., 2012). In situ ground surface C efflux has been mostly measured with dynamic and static chamber methods in the Arctic (Elberling & Brandt, 2003; Oechel et al., 1995, 2000; Oberbauer et al., 2007; Olivas et al., 2010; Welker et al., 2000; Zona et al., 2011). These widely utilized, chamber-based flux measurements can directly detect the overall gas flux from the soil surface. Although chamber-based approaches have been favored in the past and remain as considerable importance to C flux studies, there remain significant well-detailed limitations to chamber-based soil flux methodologies (Davidson & Navarro et al., 2002; Subke et al., 2009). Although much work has been done to account for, minimizing the limitations of chamber approaches and alternative methodologies, such as direct measurement of soil (CO_2) and soil diffusivity, may offer a promising alternative for quantifying C fluxes, especially in harsh, remote environments (Maier & Schack-Kirchner, 2014; Norman et al., 1997).

The difficulty of gathering soil C measurements throughout the year in the Arctic has been resulted in intermittent measurements; although automated dynamic chamber systems have been developed recently, these techniques are generally not yet practical for operations during the Arctic winter (Björkman, Morgner, Cooper et al., 2010). Frost formation, snow accumulation, and freezing temperatures often damage or disable mechanical parts of automatic systems and make chamber measurements very challenging (Bowling & Massman, 2011). The presence of the chamber, coupled with altered flux resistance from altered above ground snowpack, further complicates interpretation of many winter chamber studies in the Arctic (Kim et al., 2007; Panikov & Dedysh, 2000). Thus, below-ground concentration measurements can help in understanding year-round soil (CO_2) dynamics and identify changes throughout the year particularly during the understudied freeze-up period. It is most relevant to couple these measurements with ecosystem scale fluxes throughout the year, to be able to best identify the larger scale implications of the soil concentration dynamics (Maier & Schack-Kirchner, 2014).

In this study, nearly continuous measurements of soil (CO_2) were conducted from June 2005 to June 2007 at different depths in the soil across two sites where two eddy covariance (EC) towers were also recording ecosystem scale C fluxes. These measurements of soil (CO_2) allowed investigating the changes in the below ground concentration and environmental controls on the Arctic soil (CO_2) dynamics, while EC fluxes allowed assessing the relationship between soil processes and larger scale ecosystem fluxes.

2. Methods

2.1. Site Description

The study site is located near Utqiaġvik (formerly known as Barrow), Alaska (Figure 1). The study site is located in a naturally drained thaw lake; part of the Barrow Environmental Observatory that has been used for a water manipulation experiment (Biocomplexity in the Environment project, Zona et al., 2009), which studied the effect of the water level on the carbon balance from a drained lake (Shiklomanov et al., 2010; Sturtevant et al., 2012; Zona et al., 2011, 2009; Lipson et al., 2012). This study only includes data before the initiation of the manipulative experiment. Further details on this project and the study site are given by Zona et al. (2011, 2009).

Within the drained lake, measurements of soil (CO_2) were performed in the south section (named as Biocomplexity Experiment South, BES) in proximity of a low center polygon and in the central section (named as Biocomplexity Experiment Central, BEC) in proximity of a polygon rim. Soil parent materials in the Barrow region are marine sediments of the Pleistocene age that have been reworked by thaw-lake processes (Sellmann & Brown, 1973). The organic C content in the top 100 cm of these soils ranges from 37 to 139 kg m^{-3} (Bockheim et al., 2004), and soil bulk density of the organic layer in the study site is 0.06 g cm^{-3} on average (Lipson et al., 2013). Much of the study site is patterned ground with many polygons, producing microtopographical and hydrological heterogeneity, where polygon rims (BEC) are associated with a lower water table and drier conditions, and low-centered polygons centers (BES) and troughs have a higher water table and wetter conditions (Brown et al., 1980; Wilkman et al., 2018; Zona et al., 2011). As determined by ^{14}C dating, the soil age of the drained lake site of this study is classified as a “medium” age (50–300 YBP, Hinkel et al., 2003); within the drained lake, soil pH values range from 5.1 at the low center polygons to 4.5 at polygon rims (Hinkel et al., 2003; Lipson et al., 2012).

The Gelisol soils of BES and BEC are characterized by an organic-rich surface layer, an underlying horizon of silty clay/silt loams, and a lower organic rich mineral layer (Bockheim et al., 1999; Brown et al., 1980).

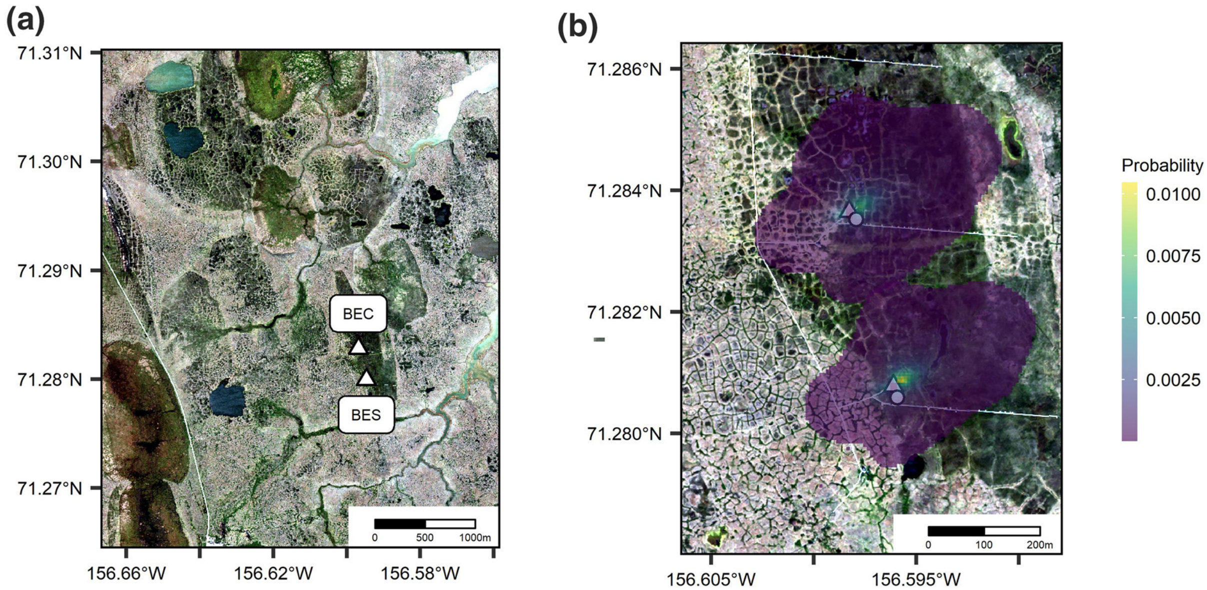

Figure 1. Overview of the experiment sites in the Barrow Environmental Observatory. The eddy covariance (EC) towers are represented by white triangles for BEC and BES (a). The location of the soil (CO_2) profiles are shown by white circles (b). The probability of the flux origin estimated from the EC towers is shown in 6 × 6 m pixels (estimated according to Kormann and Meixner [2001]), and the area shown represents 90% of the estimated flux area. Imagery from WorldView-3 was collected July 24, 2016 (Maxar Technologies). BEC, Biocomplexity Experiment Central; BES, Biocomplexity Experiment South.

Vascular plants generally dominate low-centered polygons while nonvascular plants dominate polygon rims (Hinkel et al., 2003; Olivas et al., 2010). *Sphagnum* mosses and lichens generally dominate the polygon rims in BEC, while graminoids and sedges (*Carex aquatilis*, *Eriophorum vaginatum*, and *Dupontia fisheri*) generally dominate low-centered polygons in BES; differences in vegetation community composition are generally attributed to the differences between water table and hydrological heterogeneity across these sites (Zona et al., 2009). More details about the polygon rim, the low center polygons (and other microtopographic features), are available in a variety of previous studies (S. J. Davidson et al., 2016; Liljedahl et al., 2016; Taş et al., 2018; Wainwright et al., 2014; Wilkman et al., 2018; Zona et al., 2011).

2.2. Soil CO_2 Probe Design and Installation

Soil (CO_2) was measured in each of the plots with an open-path IRGA with a probe (GMP221 and 222, Vaisala Inc., Finland) connected with a cable to a transmitter (GMT220, Vaisala Inc., Finland). These sensors have been well utilized in a variety of environments, including related peatland systems (Dinsmore et al., 2009; Dyson et al., 2011). The GMP220 series probes can detect a wide range of (CO_2), up to an in situ maximum of 20%. To detect dissolved (CO_2) in water, the sensors were installed in PVC encasements with PTFE CO_2 permeable waterproof filters (GMP343FILTER, Vaisala Inc., Finland). Due to the high soil moisture content, especially right after snow melt, these PTFE filters were encased in a plastic tape, leaving only the bottom 2 cm exposed (Figure 2a) to prevent water damage. Another encasement with PTFE filters (Porous PTFE Sheet, Small Parts Inc.) was used for probe measurements from September 20, 2006 to June 1, 2007 to prevent damage during the soil freezing (Figure 2b).

Thermal effects of the infrared beam from the CO_2 sensors can be significant when the infrared beam is emitted continuously (Jassal et al., 2004; Takagi et al., 2005). This artificial heating may enhance microbial activity, resulting in an overestimation of soil respiration. Thus, to measure any temperature fluctuations type-T thermocouples were attached to the outside of the encasements of the CO_2 probes upon installation in the soil. When the infrared beam was turned on, the encasement temperatures increased by 0.5°C in summer, but there was no detectable change in winter. As the encasement temperatures also differed by less than 0.5°C, on average, in comparison to nearby soil temperatures, any artificial temperature increase due to continuous infrared beam operation was deemed to be insignificant to the respiratory flux processes and results of this study.

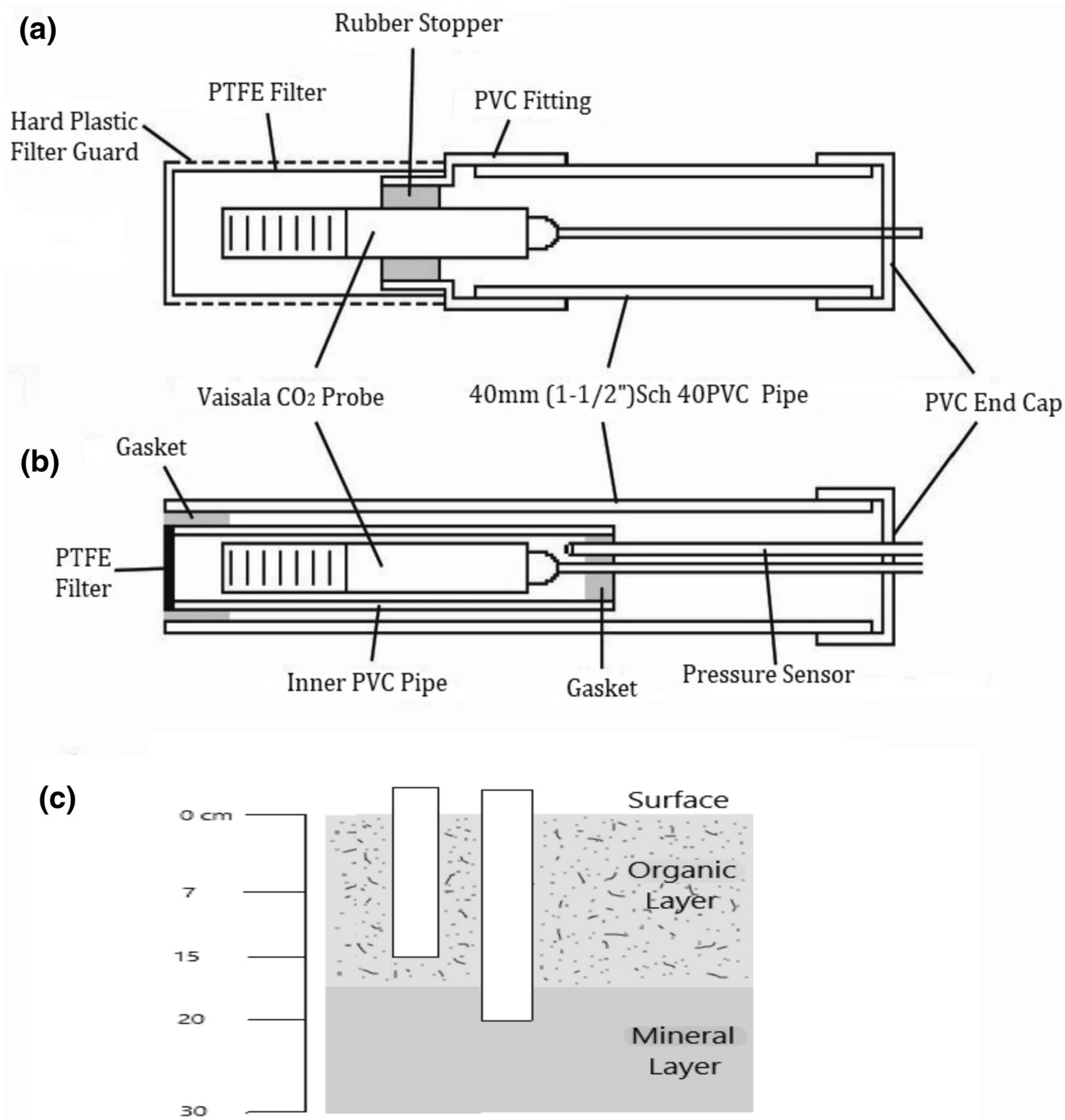

Figure 2. CO_2 probe encasements (a: used between June 2005 and August 2006, b: used between late September 2006 and June 2007) and CO_2 probe installation (c). The original encasement was used for the ground surface probe throughout the study period in both the BES and BEC sites. The probes were inserted 10 m away from the eddy covariance towers. BEC, Biocomplexity Experiment Central; BES, Biocomplexity Experiment South.

2.3. Field Measurement of Soil (CO_2)

At the end of June 2005, the Vaisala GMT222 soil probes were installed at the ground surface, in the organic layer (15 cm) and the mineral layer (20 cm) in a total of two plots to examine the contributions of CO_2 release from each soil horizon (Figure 2c). To limit disturbance of soil structure and interference between sensors, the probes were oriented vertically in the soil and spaced at least 30 cm apart horizontally. An electric drill with a hole saw drill bit of 5 cm diameter was used for sensor installation into the frozen. Damaged soil CO_2 sensors at depths of 15 and 20 cm were replaced in the beginning of September 2005 and July 2006, and in the middle of September 2006 with sensors with increased measurement range capacity. During removal, plastic caps were installed to prevent any significant gaseous emission. Overall, data retrieval was 85%, and sensor malfunction and equipment failure, January–May 2006, resulted in less than 15% data loss.

As the CO_2 probes used in this study are affected by ambient pressure and temperature, the correction developed by Tang et al. (2003) was used for GMT222 probes, and the following Equations 1–6 were used to estimate CO_2 concentration for GMT221 probes (Vaisala Inc., personal communication).

$$ci + 1 = c1 - kP1 \times \left(\frac{(p - 1013)}{1013} \right)^2 - kP2 \times \left(\frac{(p - 1013)}{1013} \right) \times p, \tag{1}$$

$$-kT1 \times \left(\frac{(25 - T)}{25} \right)^3 - kT2 \times \left(\frac{(25 - T)}{25} \right)^2 - 16320 \times (-(kT3 + kT3) \times \left(\frac{(25 - T)}{25} \right),$$

where $i = 1, 2, 3, 4$, c_1 is the uncompensated reading (ppm), p is the ambient air pressure (hPa), T is the ambient temperature (°C) and

$$kP_1 = A_{P1} \times c_i^4 + B_{P1} \times c_i^3 + G_{p1} \times c_i^2 + H_{p1} \times c_i, \tag{2}$$

$$kP_2 = A_{P2} \times c_i^3 + B_{P2} \times c_i^2 + G_{p2} \times c_i, \tag{3}$$

$$kT_1 = A_{T1} \times c_i^3 + B_{T1} \times c_i^2 + G_{T1} \times c_i + H_{p1}, \tag{4}$$

$$kT_2 = A_{T2} \times c_i^2 + B_{T2} \times c_i, \tag{5}$$

$$kT_3 = A_{T3} \times c_i^3 + B_{T3} \times c_i^2 + G_{T1} \times c_i, \tag{6}$$

where

$A_{P1} = 0.97501$, $A_{T1} = 0.046481$ and $A_{T3} = 8.3600 \times 10^{-5}$,

$B_{P1} = -54.1519$, $B_{T1} = -1.02280$ and $B_{T3} = -2.4199 \times 10^{-3}$,

$G_{P1} = 479.778$, $G_{T1} = -37.4433$ and $G_{T3} = 0.066814$,

$H_{P1} = -11362.8$ and $H_{T1} = -49.000$, and

$A_{P2} = -9.3269 \times 10^{-3}$, $A_{T2} = -3.0166$, $B_{P2} = 0.14345$, $B_{T2} = -8.8421$ and $G_{P2} = 15.7164$.

The form of Equation 1 was discovered by fitting trial curves for the experimental data of $c1$(p) and $c1$(T) at various CO_2 concentrations on the condition that kP and kT are increasing functions of CO_2 concentration through the whole pressure and temperature range. In the first iteration loop ($i = 1$), c_2 is calculated from Equation 1 by using $c1$ for Equations 2 and 3. Thenceforth, c_2 is used in the following loop ($i = 2$) to solve new values of kP and kT from Equations 2 and 3 for Equation 1. The iteration is continued until the last c_i, or c_5, is calculated and then is the pressure and temperature corrected reading. In Equation 1, c_i and c_1 are in ppm but c_i in Equations 2–6 are in percent CO_2. These equations are applicable for conditions of −20–60°C and 700–1,300 hPa, and these conditions during this experiment were within this range.

2.4. Environmental Variables

Differential type pressure transducers (PX170-07DV, Omega Engineering, Connecticut, USA) were installed at each section in the middle of September 2006 to measure the difference in pressure between the soil and the atmosphere. These data cover the last half of our study. One end of the small vinyl tube (2.5 mm diameter) was encased with the soil CO_2 sensor at each depth, and the other end was connected to the pressure sensor located at a height of 1 m above the ground. Ground pressure sensors from adjacent EC towers were used for pressure monitoring before installation of the differential type pressure transducers, and values were broadly consistent when the data periods overlapped.

Air temperature was measured by a Vaisala HMP45 sensor, protected with the ABS plastic shield, at 1.6 m above the ground and soil temperatures were measured by thermocouples at depths of 0, 5, 10, 15, 20, and 30 cm at each section. Tower soil temperatures were available only for growing seasons at BEC, while BES had year-round coverage. Tower-based soil temperatures were chosen due to their thermal stability, unlike the Vaisala adjacent thermocouples that could be influenced by sensor heating, as mentioned in Section 2.2. Although there were large gaps in tower BEC temperatures through the winter, tower temperatures were stable across sites, and so tower-based soil temperatures were used for time series and statistical analyses (Figure S1). Soil moisture was measured with a water content reflectometer (CS616, Campbell Scientific) in near proximity of the Vaisala CO_2 probes. Sensors were inserted at an angle into organic (0–10 cm) and mineral (10–20 cm) layers, and measurements were converted into percent liquid saturation adjusting for soil bulk density. All the environmental sensors were installed in summer 2005. All meteorological data were collected at 0.10 Hz and time-averaged half-hourly via a data logger (CR23X, Campbell Scientific). Thaw depths were measured every 10 m along a 200 m transect across each section during summer 2005. This transect was further extended to 300 m in the summer 2006.

2.5. EC Measurements

Ecosystem scale CO_2 fluxes measured via EC towers were used for this study in two sections of a drained lake: central (BEC, 71.28N, −156.59W) and south (BES, 71.28N, −156.59W). These two EC towers were installed in July 2005 for a water manipulation experiment (see Zona et al., 2009 for details), which started in summer 2007 and which planned to drain the BEC section and leave the BES section as control. CO_2 and H_2O fluxes were measured with an open path infrared analyzer (LI-7500, Li-COR, Lincoln NE, USA) with a sampling rate of 10Hz (Zona et al., 2009), positioned 10 cm from the center of the sonic anemometer (Wind-MasterPro, Gill Instruments Ltd., Lymington, Hampshire, UK), used to measure the three wind velocity components and the high-speed temperature fluctuations. As described in Zona et al. (2009), CO_2 and H_2O were calibrated every 2–4 weeks with ultra-high purity nitrogen and 729 ppm CO_2 in air standard gas (certified grade ± 1 ppm; Matheson Gas Product, Montgomeryville PA, USA). A dew point generator (LI-610, Li-COR, Lincoln NE, USA) was used to calibrate the H_2O vapor (Zona et al., 2009). Fluxes were computed at half-hourly resolution by means of the Eddy Pro® Software package. To smooth out the flux patterns, a 7-days running average was also computed for tower fluxes after initial processing, although nonsmoothed fluxes were also computed (Figure S1). Eddy Pro® was run including analytical spectral corrections to compensate both high-pass and low-pass spectral losses, de-spiking, Burba corrections that are most necessary during the winter compared to the summer, as described in Oechel et al. (2014), and QA/QC procedures according to Foken et al. (2004).

2.6. Statistical Analysis

To address temporal and spatial pseudoreplication, the relative importance of environmental variables in explaining growing season soil (CO_2) was determined using a linear mixed effects model (nlme package in R, Pinheiro et al., 2020). The mixed model included the fixed effects (soil temperature and the soil (CO_2) at 15 and 20 cm depth, where both parameters were measured for each depth), and random effects include date (temporal random effect) and depth nested in site (categorical random effects). Only the soil temperature at BES was used in the model due to the much better data coverage and near identical temperature trends. Correlations were tested to ensure data were comparable between sites (Figure S1). The natural log of the soil (CO_2) was used to make a linear relationship with soil temperature. Model residuals were tested for normality (Figure S2). Model performance was evaluated on the marginal coefficient of determination (similar to the explanatory power of the linear models) for generalized mixed effects models as output by the R^2 generalized linear mixed model (GLMM) function within the MuMIn package in R (Bartoń, 2020). This R^2 GLMM function was used to estimate both the marginal R^2, which describes the percentage of the variance in the respiration explained by fixed effects, and conditional R^2, which describes the percentage of the variance explained by both fixed and random effects. Differences in the temperature response between sites was tested using analysis of covariance (ANCOVA). All statistical analyses were carried out in the statistical software R, version 3.5.2 (R Core Team, 2018).

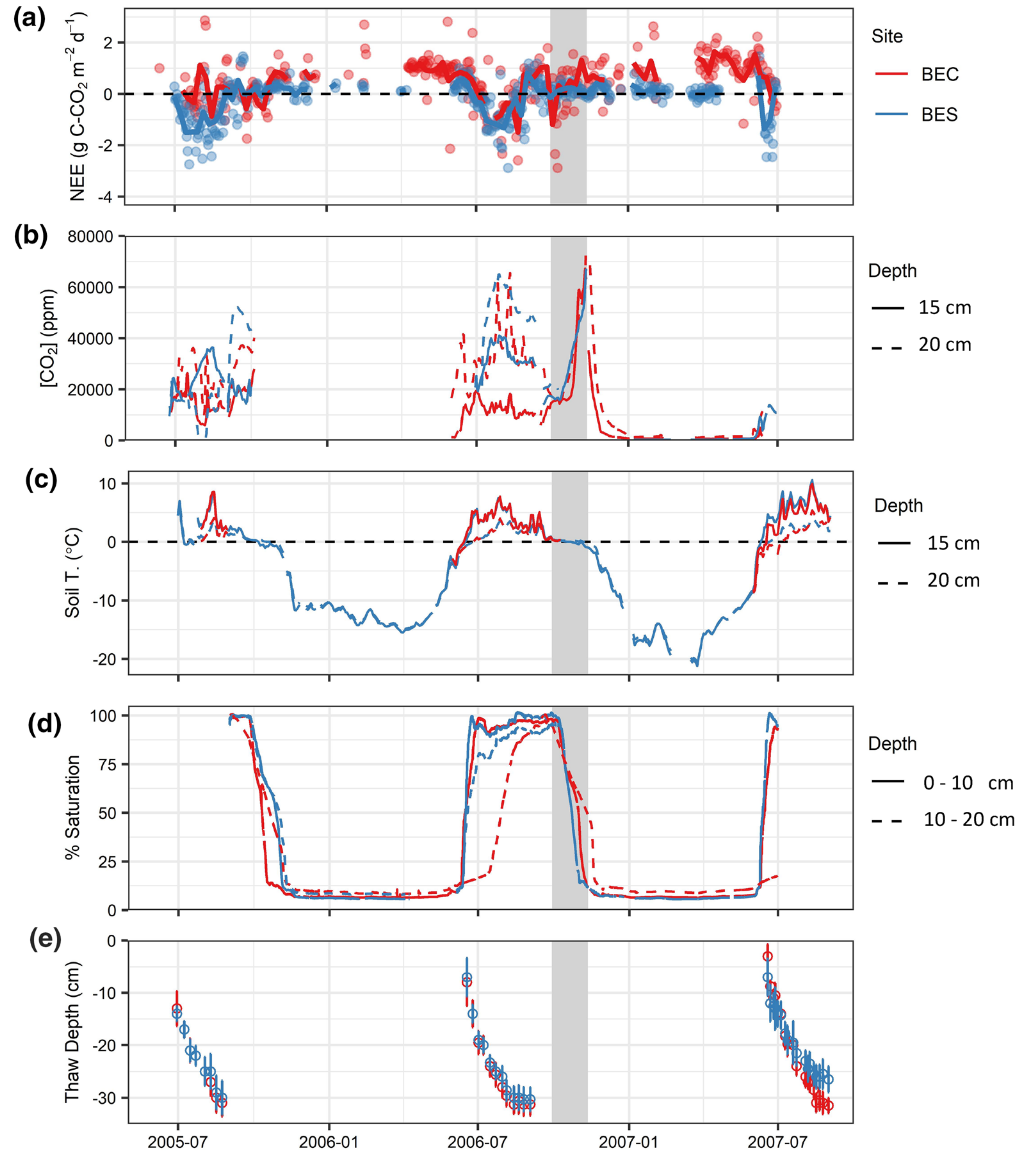

Figure 3. Temporal pattern in tower fluxes (a), soil (CO_2) (b), soil temperature (c), percent liquid saturation (d), and thaw depth (e) at the BEC and BES site from June 2005 to June 2007. Values are a daily mean except for thaw depth where it is a median ± sd. Shaded regions represent the zero-curtain period. BEC, Biocomplexity Experiment Central.

3. Results

3.1. Environmental Conditions

At BEC, median ± sd thaw depths were −24.6 ± 4.6 cm and −26.0 ± 5.5 cm in 2005 and 2006, respectively (Figure 3). In BES, median ± sd thaw depths were −24.4 ± 4.5 cm and −26.2 ± 4.2 cm during the growing season between 2005 and 2006 (Figure 3). Mean ± sd annual growing season soil temperature at 10 cm depth was on average 5.9°C ± 3.3°C and 2.3°C ± 5.0°C in BEC in 2005 and 2006, respectively. In BES, mean ± sd soil temperatures averaged 4.9°C ± 3.6°C and 4.1°C ± 7.8°C in 2005 and 2006. At BES, mean ± sd percent liquid saturation reached near complete saturation at 99% ± 0.08% during the summer in 2005 and greater than 97 ± 0.1% during the summer in 2006. At BEC, mean ± sd percent liquid saturation reached 98 ± 0.6% during the summer in 2005 and 97 ± 0.08% during the summer in 2006. On average, liquid saturation was similar between the two sites yet slightly lower at BEC than BES (Figure 3).

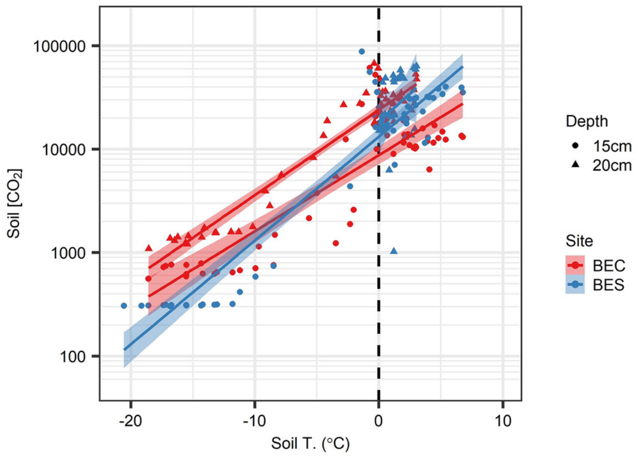

Figure 4. Relationship between weekly averaged soil (CO_2) and soil temperature. There was a significant relationship shown by the mixed-effects model with BES having a more sensitive temperature response shown by the ANCOVA. ANCOVA, analysis of covariance; BES, Biocomplexity Experiment South.

The soil temperature and liquid saturation during the summer and freezing period showed a similar pattern in both sites (BEC & BES, Figure 3); the progressive temperature increase during the growing season resulted in soil thawing and an increase in soil moisture at both sites. After the end of the summer, liquid saturation decreased progressively in the fall and winter with soil freezing (Figure 3).

3.2. Soil (CO_2) and Ecosystem Scale CO_2 Fluxes

Soil (CO_2) generally increased during the summer with increasing soil temperature (Figure 4), increasing depth of thaw and increasing soil moisture (associated with soil thawing, Figure 3). Of all the variables tested, temperature had the strongest correlation with soil (CO_2) across both sites (Table 1, Figure 4). The low-centered BES had a greater response to soil temperature variations than BEC (Table 2, Figure 4).

During the summer months, soil (CO_2) was generally an order of magnitude higher than in the atmosphere, mostly above 1% (i.e., > 10,000 ppm) at depths of 15 and 20 cm and the maximum (CO_2) at the depth of 20 cm was 3.5% (2005) and 6.5% (2006) at BEC (Figure 3). At BES, soil (CO_2) was always above 1% at the depth of 15 cm, reaching a maximum of 3.4% in 2005 and 4.1% in 2006. On average, concentrations ranged from 2.08% ± 0.84% and 1.13% ± 0.41% during the summer (June–August) in BEC between 2005 and 2006, respectively. In BES, concentrations averaged 2.36% ± 1.26% and 3.23% ± 0.55% during the summer (June–August) in 2005 and 2006. With the progressive soil freezing soil (CO_2) at both 15 and 20 cm increased to 1.80% ± 0.22% in BEC and 6.40% ± 0.19% in BES during November 2006 (Figure 3), before a steep decline cooccurring through soil freezing (Figure 3). After this steep decline, the soil (CO_2) was much lower than during the summer and freezing period and remained at 458 ± 5.41 ppm in BEC and 431 ± 5.45 ppm at BES until the following spring, when it started increasing again with soil thawing.

The ecosystem scale CO_2 fluxes measured with EC in both the BEC and BES sites did not show a significant increase concomitant with the steep increase in soil (CO_2) observed in November and December 2006 (Figure 3). Unfortunately, data loss during the remaining cold season measurements periods (i.e., Fall, 2005, 2007) did not allow us to test if these patterns were consistent across years; nonetheless, these trends were consistent across the two sites. Overall, the ecosystem scale measurements showed a consistent CO_2 loss without any pulse emissions when soil (CO_2) increased (Figure 3).

4. Discussion

4.1. Environmental Controls and Temporal Patterns in Soil (CO_2)

Soil (CO_2) observed in this study were much greater than in situ measurements of soil (CO_2) in heath in Greenland but were comparable to the dissolved (CO_2) when soil samples were thawed at the room temperature (Elberling & Brandt, 2003). Raz-Yaseef et al. (2017) found similar patterns in soil (CO_2) to our study with a rise during the summer, tailing off in the late growing season and a large peak in the fall. Soil (CO_2) was also much greater than values gathered in an Alaskan boreal forest floodplain, during both the winter and summer (Billings et al., 1998). Concentration spikes were also noted in upland tundra in central Alaska, attributed to changes in soil properties during the winter (Lee et al., 2010).

Table 1
Linear Mixed Effect Model of the Relationship Between Log of Soil (CO_2) and Soil Temperature in BES at Above (a) and Below (b) Freezing Temperatures; soil = soil, r2m = marginal r^2, and r2c = conditional r^2

Log (CO_2) ~ soil	Value	Std. error	*df*	*p*-value
(Intercept)	9.6514	0.1339	187	**<0.0001**
Soil	0.1922	0.0082	187	**<0.0001**
–	–	*r2m* = 0.7538	*r2c* = 0.8421	*n* = 192

Temporal patterns in soil (CO_2) were largely affected by soil temperature and phase change (i.e., thawing of the soil during the growing season and freezing in the fall; Table 1, Figures 3 and 4). The difference in the relationship between the soil (CO_2) and temperature across the two sites could be related to the slightly drier soils of the BEC site than the BES site

Table 2
ANCOVA Model of the Relationship Between Soil (CO_2) and Soil Temperature Across Both Sites

n = 192	Values	*df*	*F*-value	*p*-value
(Intercept)	9.58312138	186	2633.3851	**<0.0001**
Soilt	0.178228	186	912.2511	**<0.0001**
Site	0.07416287	0	0.0026	NAN
Soilt:site	0.05320238	186	15.5775	**<0.0001**

ANCOVA, analysis of covariance.

(Table 2). In fact, even if the recorded soil moisture is similar among the two sites, the BEC site is characterized by more defined polygon development resulting in drier rims across the landscape (Wilkman et al., 2018; Zona et al., 2011). More dry aerobic soils are related to higher soil diffusivities and therefore faster transport of soil gas to the atmosphere (Moldrup et al., 2000). Additionally, different processes (current production or storage of previously produced CO_2) can contribute to the increase in (CO_2), which we observed at soil temperatures well below zero , and we further discuss this in the next sections.

4.2. Patterns in Soil (CO_2) and Ecosystem Scale CO_2 Fluxes

Physical processes may govern the rapid increase of CO_2 concentration seen through the fall shoulder season (Figure 3). Our soil temperature and soil moisture data suggest that the freezing process began in late September and was completed by the middle of November at the two research sites. The large increase in soil (CO_2) noted during the freezing period suggests that phase change (i.e., soil freezing) was an important factor that resulted in rising soil (CO_2) in the unfrozen zone. Percent liquid saturation at depth decreased steadily through the fall shoulder season. Throughout this freezeup period, water migrates bidirectionally to the freezing fronts leaving air pockets in the remaining active layer (Bing et al., 2015). Freezing forces dissolved CO_2 out of solution, and as such the zero-curtain would become pressurized as dissolved CO_2, salt, and ions are forced out of solution (Bing et al., 2015; Tagesson et al., 2012). The pressure accumulation and gas buildup may help contribute to the rapid rise in concentration through this period (Mastepanov et al., 2013; Pirk et al., 2015). Concentrations may also increase during the fall due to the frozen surface trapping gas at depth (Byun et al., 2017). Elberling and Brandt (2003) found high (CO_2) in freezing soils and concluded that it was mostly caused by CO_2 entrapment rather than concurrent respiration. The peak increase in soil (CO_2) with soil freezing is consistent with the conclusion by Elberling and Brandt (2003), given the lower temperatures observed during the fall (e.g., temperature being the dominant driver of soil CO_2 production; Elberling et al., 2008; Wallenstein et al., 2008). On the other hand, respiration still occurs well below freezing in Arctic soils, and we suggest this may contribute to the increase in the soil (CO_2) during the fall, although it is not possible to determine the relative influence of production and storage change processes in this study (Nikrad et al., 2016; Panikov et al., 2006). Isotopic measurements should be used to identify the origin of the CO_2 emitted in the fall and evaluate the relative importance of current production versus storage of CO_2 produced during the summer (Czimczik & Welker, 2010).

The subsurface data set collected in this study shows how soil (CO_2) progressively increases in the fall until there is a rapid decrease in soil (CO_2). The precipitous drop in soil (CO_2) observed around mid-November (BEC) and between mid-November and January (BES) may suggest rapid gas release through cracks in the soil that formed during freezing (Figure 3). Mastepanov et al. (2008), Sturtevant et al. (2012), Commane et al. (2017), and Arndt et al. (2019) have observed significant gas efflux during the freezing period, concluding that the efflux was primarily caused by release through cracks. The rapid loss of CO_2 concentration may also be influenced by other physical transport mechanisms. Turbulent wind-driven changes in atmospheric pressure can cause a pumping effect that also leads to a large-scale convective transport of CO_2 within and out of the snowpack (Björkman, Morgner, Björk et al., 2010; Bowling & Massman, 2011). The ecosystem scale measurements in this study, however, did not fully capture these peak events at all sites and at all times. It is likely that there are multiple cracks across the landscape releasing bursts of CO_2. We assume that during the years of our measurements, these release events occurred over a prolonged period. While each one can be significant locally, when released over time across the landscape, emissions are increased, but burst emission events may not be detected.

4.3. Soil (CO_2) and Ecosystem CO_2 Fluxes After Soil Freezing

Soil respiration has been readily shown to occur in frozen soils (Panikov & Dedysh, 2000; Panikov et al., 2006; Zimov, Zimova, et al., 1993) resulting in elevated soil CO_2 values. Of note, Zimov, Semiletov, et al. (1993) reported that increased aeration of deep soil layers, as a result of drying processes during freezeup, could increase soil respiration. Yanai et al. (2004) also found that thawing and freezing can significantly affect microbial activity, while Watanabe and Ito (2008) noted the possibility of microbial migration via micro-channel soil water flow, due to ice exclusion near the freezing front. Arctic microbes have been found to be active during the wintertime, and research has found that measurable microbial growth and respiration can continue at significant levels well below zero temperatures (Drotz et al., 2010; Jansson & Taş, 2014; McMahon et al., 2009; Panikov et al., 2006; Townsend-Small et al., 2017). Thus, significant microbial activity is not precluded in subzero temperatures or in frozen soils, and this activity could readily affect concentrations in these soils; especially if loss from the soil column is precluded by a more or less impervious frozen layer at the soil surface. It is interesting to note that in the early fall, there appears to be a decrease in soil diffusivity, relative to production, that results in a significant build up in soil (CO_2) over a period of 4–6 weeks followed by a similarly rapid decrease in soil concentration around mid-November. We assume that this build up and release occurs at a time of changing surface diffusivities and a changing balance between production and transport. Thus, biotic and abiotic processes seem to be vital to biogeochemical dynamics in the fall shoulder season.

Soil (CO_2) increased rapidly in the soil during the fall shoulder season, but while concentrations dropped quickly thereafter, ecosystem CO_2 fluxes did not capture significant burst emissions. Soil CO_2 could be pushed further into the zero-curtain as soils freeze, which, unfortunately, we were not able to capture given the current experimental design. However, the consistent ecosystem scale CO_2 loss during the winter, when the soil (CO_2) is very low, suggests a slow release of current production of soil CO_2 from soil respiration. Soil (CO_2) reached levels of ∼75,000 to 100,000 ppm in the soil in mid-November. Assuming a frozen upper 15 cm and an unfrozen soil zone from 15 to 30 cm, a pore space of <50%, and assuming a half atmosphere/half water zone with a 50% liquid saturation, the total amount of CO_2 stored at the end of the zero curtain in this layer is 7.7 g C- CO_2 m^{-2}. If this is released over ten days in the fall, this would increase soil fluxes by 0.8 g m^{-2} d^{-1}. It is not currently possible to parse the fall fluxes and conclude, definitively, that fall fluxes are increased by this amount concomitant with the outgassing of soil CO_2, but fluxes in BEC strongly fit this pattern during freezeup with emissions also averaging 0.8 g m^{-2} d^{-1} in the last two weeks of November, suggesting the soil concentration record is consistent with the tower flux patterns (Figure 3). Given the decrease in [CO_2] in the fall and winter, this supports studies that show spring emissions are likely due to the revitalization of the microbial community during snow melt (Arndt et al., 2020). Abiotic factors may also be important in driving a lag in the emission of CO_2 trapped in the soil prior to the rapid degassing in November. Pressure and temperature are important controlling variables that can affect the diffusion and mass transport of CO_2 out of the soil (Euskirchen et al., 2017; Webb et al., 2016). On the other hand, temporal factors are also important, as CO_2 peak emissions can vary by year, active layer depth and by exchange events mediated by wind-driven pressure fluctuations (Lüers et al., 2014; Mastepanov et al., 2013; Zona et al., 2016).

Winter carbon dynamics are quite complex, and the intersection between temperature response, growing season productivity, and transport functions will drive future loss pathways (Liu et al., 2018). Understanding the dynamics occurring during the long Arctic winter is critical as these periods cover the majority of the year and can contribute significantly to the annual CO_2 emissions. The significant fall and early winter emissions reported by the EC system may suggest a gradual release of trapped CO_2 over the fall and early winter (Commane et al., 2017; Sturtevant et al., 2012). The low soil (CO_2) after November suggests either a very low respiration rate after freezing of the entire soil column, changes in the continued contributions from stored CO_2, or efficient transport of respired CO_2 to the atmosphere, possibly through cracks and channel in the frozen soil, for example along roots and stem bases (Rains et al., 2016; Roland et al., 2015).

5. Conclusions

Soil (CO_2) in the active layer are predominantly controlled by physical factors, such as temperature and thawing and freezing (phase change), and by biological factors, such as respiration of plants and microbes. Soil (CO_2) and ecosystem scale CO_2 loss increased as thaw depth increases at the beginning of the thawing period, and concentrations also increased in the unfrozen active layer when soils began to freeze in the fall. Through the fall, landscape level emissions showed a steady and continuous release of soil (CO_2) to the atmosphere. Measuring soil (CO_2) dynamics and ecosystem scale CO_2 fluxes is critical to understand the response of Arctic ecosystems to warming. In the future, changes in soil (CO_2) could be coupled with point-based chamber measurements of soil fluxes. Further, isotopic measurements could be used to characterize the origin of the carbon released to the atmosphere at different seasons.

Data Availability Statement

Data for all figures and tables can be accessed in the NSF Arctic Data Center via the link *urn:uuid:e5e4b-caf-d82c-421c-be21-8f24521204a8*. Geospatial support for this work was provided by the Polar Geospatial Center under NSF OPP award 1204263, and 1702797. This research was conducted on land owned by the Ukpeagvik Inupiat Corporation (UIC).

Acknowledgments
This work was funded by the Office of Polar Programs of the National Science Foundation (NSF) awarded to DZ, WCO, and DAL (award number 1204263) with additional logistical support funded by the NSF Office of Polar Programs, and by the Carbon in Arctic Reservoirs Vulnerability Experiment (CARVE), an Earth Ventures (EV-1) investigation, under contract with the National Aeronautics and Space Administration, and by the ABoVE (NNX-15AT74A; NNX16AF94A) Program. This project has received funding from the European Union's Horizon 2020 research and innovation program under the grant agreement No. 727890, from the and by the Natural Environment Research Council (NERC) UAMS Grant (NE/P002552/1), and from the NOAA Cooperative Science Center for Earth System Sciences and Remote Sensing Technologies (NOAA-CESSRST) under the Cooperative Agreement Grant # NA16SEC4810008.

References

Arctic Climate Impact Assessment. (2004). *Impacts of a warming Arctic—Arctic climate impact assessment*. Cambridge, UK: Cambridge University Press.

Arndt, K. A., Lipson, D. A., Hashemi, J., Oechel, W. C., & Zona, D. (2020). Snow melt stimulates ecosystem respiration in Arctic ecosystems. *Global Change Biology*, *26*, 5042–5051. https://doi.org/10.1111/gcb.15193

Arndt, K. A., Oechel, W. C., Goodrich, J. P., Bailey, B. A., Kalhori, A., Hashemi, J., et al. (2019). Sensitivity of methane emissions to later soil freezing in Arctic tundra ecosystems. *Journal of Geophysical Research: Biogeosciences*, *124*, 2595–2609. https://doi.org/10.1029/2019JG005242

Banin, A., & Anderson, D. M. (1974). Effects of salt concentration changes during freezing on the unfrozen water content of porous materials. *Water Resources Research*, *10*, 124–128. https://doi.org/10.1029/WR010i001p00124

Bartoń, K. (2020). *MuMIn: Multi-Model inference. R package version 1.43.17*. Retrieved from https://CRAN.R-project.org/package=MuMIn>

Belshe, E. F., Schuur, E. A., & Bolker, B. M. (2013). Tundra ecosystems observed to be CO_2 sources due to differential amplification of the carbon cycle. *Ecology Letters*, *16*(10), 1307–1315. https://doi.org/10.1111/ele.12164

Billings, W. D., Luken, J. O., Mortesen, D. A., & Peterson, K. M. (1983). Increasing atmospheric carbon dioxide: possible effect on arctic tundra. *Oecologia*, *58*, 286–289. https://doi.org/10.1007/BF00385225

Billings, W. D., Richter, D. D., & Yarie, J. (1998). Soil carbon dioxide fluxes and profile concentrations in two boreal forests. *Canadian Journal of Forest Research*, *28*, 1773–1783. https://doi.org/10.1139/x98-145

Bing, H., He, P., & Zhang, Y. (2015). Cyclic freeze–thaw as a mechanism for water and salt migration in soil. *Environmental Earth Sciences*, *74*(1), 675–681. https://doi.org/10.1007/s12665-015-4072-9

Björkman, M. P., Morgner, E., Björk, R. G., Cooper, E. J., Elberling, B., & Klemedtsson, L. A. (2010). Comparison of annual and seasonal carbon dioxide effluxes between sub-Arctic Sweden and high-Arctic Svalbard. *Polar Research*, *29*(1), 75–84. https://doi.org/10.1111/j.1751-8369.2010.00150.x

Björkman, M. P., Morgner, E., Cooper, E. J., Elberling, B., Klemedtsson, L., & Björk, R. (2010). Winter carbon dioxide effluxes from Arctic ecosystems: An overview and comparison of methodologies. *Global Biogeochemical Cycles*, *24*, GB3010. https://doi.org/10.1029/2009GB003667

Bockheim, J. G., Everett, L. R., Hinkel, K. M., Nelson, F. E., & Brown, J. (1999). Soil organic carbon storage and distribution in arctic tundra, Barrow, Alaska. *Soil Science Society of America Journal*, *63*(4), 934–940. https://doi.org/10.2136/sssaj1999.634934x

Bockheim, J. G., Hinkel, K. M., Eisner, W. R., & Dai, X. Y. (2004). Carbon pools and accumulation rates in an age-series of soils in drained thaw-lake basins, Arctic Alaska. *Soil Science Society of America Journal*, *68*(2), 697–704. https://doi.org/10.2136/sssaj2004.6970

Bowling, D. R., & Massman, W. J. (2011). Persistent wind-induced enhancement of diffusive CO_2 transport in a mountain forest snowpack. *Journal of Geophysical Research*, *116*(G4), G04006. https://doi.org/10.1029/2011JG001722

Brown, J., Everett, K. R., Webber, P. J., MacLean, S. F., & Murray, D. F. (1980). The coastal tundra at Barrow, Alaska. In J. Brown, P. C. Miller, L. L. Tieszen, & F. L. Bunnell (Eds.), *An arctic ecosystem* (pp. 1–29). Stroudsburg, Pennsylvania: Dowden Hutchinson and Ross.

Byun, E., Yang, J. W., Kim, Y., & Ahn, J. (2017). Trapped greenhouse gases in the permafrost active layer: preliminary results for methane peaks in vertical profiles of frozen Alaskan soil cores. *Permafrost and Periglacial Processes*, *28*(2), 477–484. https://doi.org/10.1002/ppp.1935

Chapman, W. L., & Walsh, J. E. (1993). Recent variations of sea ice and air temperature in high latitudes. *Bulletin of the American Meteorological Society*, *74*, 33–47. https://doi.org/10.1175/1520-0477(1993)074<0033:RVOSIA>2.0.CO;2

Christensen, J. H., Kanikicharla, K. K., Aldrian, E., An, S. I., Cavalcanti, I. F. A., de Castro, M., et al. (2013). Climate phenomena and their relevance for future regional climate change. In T. F. Stocker, D., Qin, G-K., Plattner, M., Tignor, S. K., Allen, J., Boschung, A., Nauels, et al. (Eds.), *Climate change 2013: The physical science basis. Contribution of working Group 1 to the Fifth assessment report of the intergovernmental panel on climate change*. Cambridge, UK: Cambridge University Press.

Commane, R., Lindaas, J., Benmergui, J., Luus, K. A., Chang, R. Y., Daube, B. C., et al. (2017). Carbon dioxide sources from Alaska driven by increasing early winter respiration from Arctic tundra. *Proceedings of the National Academy of Sciences*, *114*(21), 5361–5366. https://doi.org/10.1073/pnas.1618567114

Coxson, D. S., & Parkinson, D. (1987). Winter respiratory activity in aspen woodland forest floor litter and soils. *Soil Biology and Biochemistry*, *19*, 49–59. https://doi.org/10.1016/0038-0717(87)90125-8

Czimczik, C. I., & Welker, J. M. (2010). Radiocarbon content of CO_2 respired from high Arctic tundra in northwest Greenland. *Arctic, Antarctic, and Alpine Research*, *42*(3), 342–350. https://doi.org/10.1657/1938-4246-42.3.342

Davidson, K. V. S., Verchot, L. V., & Navarro, R. (2002). Minimizing artifacts and biases in chamber-based measurements of soil respiration. *Agricultural and Forest Meteorology*, *113*(1), 21–37. https://doi.org/10.1016/S0168-1923(02)00100-4

Davidson, S. J., Sloan, V. L., Phoenix, G. K., Wagner, R., Fisher, J. P., Oechel, W. C., & Zona, D. (2016). Vegetation type dominates the spatial variability in CH_4 emissions across multiple arctic tundra landscapes. *Ecosystems*, *19*(6), 1116–1132. https://doi.org/10.1007/s10021-016-9991-0

Dinsmore, K. J., Billett, M. F., & Moore, T. R. (2009). Transfer of carbon dioxide and methane through the soil-water-atmosphere system in Mar Bleue peatland, Canada. *Hydrological Processes*, *23*, 330–341. https://doi.org/10.1002/hyp.7158

Drotz, S. H., Sparrman, T., Nilsson, M. B., Schleucher, J., & Öquist, M. G. (2010). Both catabolic and anabolic heterotrophic microbial activity proceed in frozen soils. *Proceedings of the National Academy of Sciences*, *107*(49), 21046–21051. https://doi.org/10.1073/pnas.1008885107

Drotz, S. H., Tilston, E. L., Sparrman, T., Schleucher, J., Nilsson, M., & Öquist, M. G. (2009). Contributions of matric and osmotic potentials to the unfrozen water content of frozen soils. *Geoderma*, *148*(3–4), 392–398. https://doi.org/10.1016/j.geoderma.2008.11.007

Dyson, K. E., Billett, M. F., Dinsmore, K. J., Harvey, F., Thomson, A. M., Piirainen, S., & Kortelainen, P. (2011). Release of aquatic carbon from two peatland catchments in E. Finland during the spring snowmelt period. *Biogeochemistry*, *103*, 125–142. https://doi.org/10.1007/s10533-010-9452-3

Elberling, B., & Brandt, K. K. (2003). Uncoupling of microbial CO_2 production and release in frozen soil and its implications for field studies of the arctic C cycling. *Soil Biology and Biochemistry*, *35*, 263–272. https://doi.org/10.1016/S0038-0717(02)00258-4

Elberling, B., Nordstrøm, C., Grøndahl, L., Søgaard, H., Friborg, T., Christensen, T. R., et al. (2008). High-arctic soil CO_2 and CH_4 production controlled by temperature, water, freezing and snow. *Advances in Ecological Research*, *40*, 441–472. https://doi.org/10.1016/S0065-2504(07)00019-0

Euskirchen, E. S., Bret-Harte, M. S., Scott, G. J., Edgar, C., & Shaver, G. R. (2012). Seasonal patterns of carbon dioxide and water fluxes in three representative tundra ecosystems in northern Alaska. *Ecosphere*, *3*(1), 1–9. https://doi.org/10.1890/ES11-00202.1

Euskirchen, E. S., Bret-Harte, M. S., Shaver, G. R., Edgar, C. W., & Romanovsky, V. E. (2017). Long-term release of carbon dioxide from arctic tundra ecosystems in Alaska. *Ecosystems*, *20*(5), 960–974. https://doi.org/10.1007/s10021-016-0085-9

Fahnestock, J. T., Jones, H., & Welker, M. (1999). Wintertime CO_2: Efflux from arctic soils: Implications for annual carbon budgets. *Global Biogeochemical Cycles*, *13*(3), 775–779. https://doi.org/10.1029/1999GB900006

Fahnestock, J. T., Jones, M. H., Brooks, P. D., Walker, D. A., & Welker, J. M. (1998). Winter and early spring CO_2 efflux from tundra communities of northern Alaska. *Journal of Geophysical Research*, *103*, 29023–29027. https://doi.org/10.1029/98JD00805

Foken, T., Göockede, M., Mauder, M., Mahrt, L., Amiro, B., & Munger, W. (2004). Post-field data quality control. In X. Lee, W. Massman, & B. Law (Eds.), *Handbook of micrometeorology* (pp. 181–208). Dordrecht, Netherlands: Springer.

Grogan, P., & Chapin, F. S. (2000). Initial effects of experimental warming on above-and belowground components of net ecosystem CO_2 exchange in arctic tundra. *Oecologia*, *125*(4), 512–520. https://doi.org/10.1007/s004420000490

Henry, H. A. (2007). Soil freeze–thaw cycle experiments: trends, methodological weaknesses and suggested improvements. *Soil Biology and Biochemistry*, *39*(5), 977–986. https://doi.org/10.1016/j.soilbio.2006.11.017

Hinkel, K. M., Doolittle, J. A., Bockheim, J. G., Nelson, F. E., Paetzold, R., Kimble, J. M., & Travis, R. (2001). Detection of subsurface permafrost features with ground-penetrating radar, Barrow, Alaska. *Permafrost and Periglacial Processes*, *12*, 179–190. https://doi.org/10.1002/ppp.369

Hinkel, K. M., Eisner, W. R., Bockheim, J. G., Nelson, F. E., Peterson, K. M., & Dai, X. Y. (2003). Spatial extent, age, and carbon stocks in drained thaw lake basins on the Barrow Peninsula, Alaska. *Arctic Antarctic and Alpine Research*, *35*, 291–300. https://doi.org/10.1657/1523-0430(2003)035[0291:SEAACS]2.0.CO;2

Hinzman, L. D., Kane, D. L., Gieck, R. E., & Everett, K. R. (1991). Hydrologic and thermal properties of the active layer in the Alaskan Arctic. *Cold Regions Science and Technology*, *19*, 95–110. https://doi.org/10.1016/0165-232X(91)90001-W

Hugelius, G., Strauss, J., Zubrzycki, S., Harden, J. W., Schuur, E. A. G., Ping, C. L., et al. (2014). Estimated stocks of circumpolar permafrost carbon with quantified uncertainty ranges and identified data gaps. *Biogeosciences Discussions*, *11*, 6573–6593. https://doi.org/10.5194/bg-11-6573-2014

Jansson, J. K., & Taş, N. (2014). The microbial ecology of permafrost. *Nature Reviews Microbiology*, *12*(6), 414–425. https://doi.org/10.1038/nrmicro3262

Jassal, R. S., Black, T. A., Drewitt, G. B., Novak, M. D., Gaumont-Guay, D., & Nesic, Z. (2004). A model of the production and transport of CO_2 in soil: Predicting soil CO_2 concentrations and CO_2 efflux from a forest floor. *Agricultural and Forest Meteorology*, *124*, 219–236. https://doi.org/10.1016/j.agrformet.2004.01.013

Jones, H. G., Pomeroy, J. W., Davies, T. D., Tranter, M., & Marsh, P. (1999). CO_2 in Arctic snow cover: landscape form, in-pack gas concentration gradients, and the implications for the estimation of gaseous fluxes. *Hydrological Processes*, *13*, 2977–2989. https://doi.org/10.1002/(SICI)1099-1085(19991230)13:18<2977::AID-HYP12>3.0.CO;2-%23

Jorgenson, M. T., Racine, C. H., Walters, J. C., & Osterkamp, T. E. (2001). Permafrost degradation and ecological changes associated with a warming climate in central Alaska. *Climate Change*, *48*, 551–579. https://doi.org/10.1023/A:1005667424292

Kade, A., Bret-Harte, M. S., Euskirchen, E. S., Edgar, C., & Fulweber, R. A. (2012). Upscaling of CO_2 fluxes from heterogeneous tundra plant communities in Arctic Alaska. *Journal of Geophysical Research: Biogeosciences*, *117*(G4), G04007. https://doi.org/10.1029/2012JG002065

Kanevskiy, M., Shur, Y., Jorgenson, T., Brown, D. R., Moskalenko, N., Brown, J., et al. (2017). Degradation and stabilization of ice wedges: Implications for assessing risk of thermokarst in northern Alaska. *Geomorphology*, *297*, 20–42. https://doi.org/10.1016/j.geomorph.2017.09.001

Kerfoot, D. E. (1972). Thermal contraction cracks in an Arctic tundra environment. *Arctic*, *25*(2), 142–150.

Kim, Y., Kimball, J. S., Zhang, K., & McDonald, K. C. (2012). Satellite detection of increasing Northern Hemisphere non-frozen seasons from 1979 to 2008: Implications for regional vegetation growth. *Remote Sensing of the Environment*, *121*, 472–487. https://doi.org/10.1016/j.rse.2012.02.014

Kim, Y., Ueyama, M., Nakagawa, F., Tsunogai, U., Harazono, Y., & Tanaka, N. (2007). Assessment of winter fluxes of CO_2 and CH_4 in boreal forest soils of central Alaska estimated by the profile method and the chamber method: A diagnosis of methane emission and implications for the regional carbon budget. *Tellus B: Chemical and Physical Meteorology*, *59*(2), 223–233. https://doi.org/10.1111/j1600-0889.2006.00233.x

Koopmans, R. W., & Miller, R. D. (1966). Soil freezing and soil water characteristic curves. *Soil Science Society of America Journal*, *30*(6), 680–685. https://doi.org/10.2136/sssaj1966.03615995003000060011x

Kormann, R., & Meixner, F. X. (2001). An analytical footprint model for non-neutral stratification. *Boundary-Layer Meteorology*, *99*(2), 207–224.

Lee, H., Schuur, E. A., & Vogel, J. G. (2010). Soil CO_2 production in upland tundra where permafrost is thawing. *Journal of Geophysical Research: Biogeosciences*, *115*(G1). https://doi.org/10.1029/2008JG000906

Liljedahl, A. K., Boike, J., Daanen, R. P., Fedorov, A. N., Frost, G. V., Grosse, G., et al. (2016). Pan-Arctic ice-wedge degradation in warming permafrost and its influence on tundra hydrology. *Nature Geoscience*, *9*(4), 312–318. https://doi.org/10.1038/ngeo2674

Lipson, D. A., Raab, T. K., Goria, D., & Zlamal, J. (2013). The contribution of Fe(III) and humic acid reduction to ecosystem respiration in drained thaw lake basins of the Arctic Coastal Plain. *Global Biogeochemical Cycles*, *27*, 1–11. https://doi.org/10.1002/gbc.20038

Lipson, D. A., Zona, D., Raab, T. K., Bozzolo, F., Mauritz, M., & Oechel, W. C. (2012). Water table height and microtopography control biogeochemical cycling in an Arctic coastal tundra ecosystem. *Biogeosciences*, *9*, 1–15. https://doi.org/10.5194/bg-9-577-2012

Liu, D., Piao, S., Wang, T., Wang, X., Wang, X., Ding, J., et al. (2018). Decelerating autumn CO_2 release with warming induced by attenuated temperature dependence of respiration in northern ecosystems. *Geophysical Research Letters*, *45*(11), 5562–5571. https://doi.org/10.1029/2018GL077447

Lüers, J., Westermann, S., Piel, K., & Boike, J. (2014). Annual CO_2 budget and seasonal CO_2 exchange signals at a high Arctic permafrost site on Spitsbergen, Svalbard archipelago. *Biogeosciences*, *11*(22), 6307–6322. https://doi.org/10.5194/bg-11-6307-2014

Maier, M., & Schack-Kirchner, H. (2014). Using the gradient method to determine soil gas flux: A review. *Agricultural and Forest Meteorology*, *192*, 78–95. https://doi.org/10.1016/j.agrformet.2014.03.006

Marion, G. M., & Oechel, W. C. (1993). Mid-to late-Holocene carbon balance in Arctic Alaska and its implications for future global warming. *The Holocene*, *3*(3), 193–200. https://doi.org/10.1177/095968369300300301

Mastepanov, M., Sigsgaard, C., Dlugokencky, E. J., Houweling, S., Ström, L., Tamstorf, M. P., & Christensen, T. R. (2008). Large tundra methane burst during onset of freezing. *Nature*, *456*, 628–630. https://doi.org/10.1038/nature07464

Mastepanov, M., Sigsgaard, C., Tagesson, T., Ström, L., Tamstorf, M. P., Lund, M., & Christensen, T. R. (2013). Revisiting factors controlling methane emissions from high-Arctic tundra. *Biogeosciences*, *10*(7), 5139–5158. https://doi.org/10.5194/bg-10-5139-2013

McGuire, A. D., Christensen, T. R., Hayes, D., Heroult, A., Euskirchen, E., Kimball, J. S., et al. (2012). An assessment of the carbon balance of Arctic tundra: comparisons among observations, process models, and atmospheric inversions. *Biogeosciences*, *9*, 3185–3204. https://doi.org/10.5194/bg-9-3185-2012

McMahon, S. K., Wallenstein, M. D., & Schimel, J. P. (2009). Microbial growth in Arctic tundra soil at −2 C. *Environmental Microbiology Reports*, *1*(2), 162–166. https://doi.org/10.1111/j.1758-2229.2009.00025.x

Mikan, C. J., Schimel, J. P., & Doyle, A. P. (2002). Temperature controls of microbial respiration in arctic tundra soils above and below freezing. *Soil Biology and Biochemistry*, *34*, 1785–1795. https://doi.org/10.1016/S0038-0717(02)00168-2

Mölders, N., & Romanovsky, V. E. (2006). Long-term evaluation of the Hydro-Thermodynamic Soil-Vegetation Scheme's frozen ground/permafrost component using observations at Barrow, Alaska. *Journal of Geophysical Research*, *111*(D4), D04105. https://doi.org/10.1029/2005JD005957

Moldrup, P., Olesen, T., Schjønning, P., Yamaguchi, T., & Rolston, D. E. (2000). Predicting the gas diffusion coefficient in undisturbed soil from soil water characteristics. *Soil Science Society of America Journal*, *64*(1), 94–100. https://doi.org/10.2136/sssaj2000.64194x

Nadelhoffer, K. J., Giblin, A. E., Shaver, G. R., & Linkins, A. E. (1992). Microbial processes and plant nutrient availability in arctic soils. In F. S. Chapin, R. L. Jefferies, J. F. Reynolds, G. R. Shaver, & J. Svoboda (Eds.), *Arctic ecosystems in a changing climate* (pp. 281–300). London, UK: Academic Press.

Natali, S. M., Watts, J. D., Rogers, B. M., Potter, S., Ludwig, S. M., Selbmann, A. K., et al. (2019). Large loss of CO_2 in winter observed across the northern permafrost region. *Nature Climate Change*, *9*(11), 852–857. https://doi.org/10.1038/s41558-019-0592-8

Nikrad, M. P., Kerkhof, L. J., & Häggblom, M. M. (2016). The subzero microbiome: Microbial activity in frozen and thawing soils. *FEMS Microbiology Ecology*, *92*(6), fiw081. https://doi.org/10.1093/femsec/fiw081

Norman, J. M., Kucharik, C. J., Gower, S. T., Baldocchi, D. D., Crill, P. M., Rayment, M., et al. (1997). A comparison of six methods for measuring soil-surface carbon dioxide fluxes. *Journal of Geophysical Research: Atmosphere*, *102*(D24), 28771–28777. https://doi.org/10.1029/97JD01440

Oberbauer, S. F., Tweedie, C. E., Welker, J. M., Fahnestock, J. T., Henry, G. H. R., Webber, P. J., et al. (2007). Carbon dioxide exchange responses of arctic tundra ecosystems to experimental warming along latitudinal and moisture gradients. *Ecological Monographs*, *77*, 221–238.

Oechel, W. C., Hastings, S. J., Jenkins, M., Riechers, G., Grulke, N., & Vourlitis, G. (1993). Recent change of arctic tundra ecosystems from a net carbon dioxide sink to a source. *Nature*, *361*, 520–523. https://doi.org/10.1038/361520a0

Oechel, W. C., Laskowski, C. A., Burba, G., Gioli, B., & Kalhori, A. M. (2014). Annual patterns and budget of CO_2 flux in an Arctic tussock tundra ecosystem. *Journal of Geophysical Research: Biogeosciences*, *119*, 323–339. https://doi.org/10.1002/2013JG002431

Oechel, W. C., Vourlitis, G. L., Hastings, S. J., Ault, R. P., & Bryant, P. (1998). The effects of water table manipulation and elevated temperature on the net CO_2 flux of wet sedge tundra ecosystems. *Global Change Biology*, *4*, 77–90. https://doi.org/10.1046/j.1365-2486.1998.00110.x

Oechel, W. C., Vourlitis, G. L., Hastings, S. J., & Bochkarev, S. A. (1995). Change in arctic CO_2 flux over two decades: effects of climate change at Barrow, Alaska. *Ecological Applications*, *5*, 846–855. https://doi.org/10.2307/1941992

Oechel, W. C., Vourlitis, G. L., Hastings, S. J., Zulueta, R. M., Hinzman, L. D., & Kane, D. L. (2000). Acclimation of ecosystem CO_2 exchange in the Alaskan Arctic in response to decadal climatic warming. *Nature*, *406*, 978–981. https://doi.org/10.1038/35023137

Olivas, P. C., Oberbauer, S. F., Tweedie, C., Oechel, W. C., & Kuchy, A. (2010). Responses of CO_2 flux components of Alaskan coastal plain tundra to shifts in water table. *Journal of Geophysical Research*, *115*, G00I05. https://doi.org/10.1029/2009GOO1254

Panikov, N. S., & Dedysh, S. N. (2000). Cold season CH_4 and CO_2 emission from boreal peat bogs (West Siberia): Winter fluxes and thaw activation dynamics. *Global Biogeochemical Cycles*, *14*(4), 1071–1080. https://doi.org/10.1029/1999GB900097

Panikov, N. S., Flanagan, P. W., Oechel, W. C., Mastepanov, M. A., & Christensen, T. R. (2006). Microbial activity in soils frozen to below −39°C. *Soil Biology and Biochemistry*, *38*(4), 785–794. https://doi.org/10.1016/j.soilbio.2005.07.004

Ping, C. L., Jastrow, J. D., Jorgenson, M. T., Michaelson, G. J., & Shur, Y. L. (2015). Permafrost soils and carbon cycling. *Soil*, *1*, 147–171. https://doi.org/10.5194/soild-1-709-2014

Pinheiro, J., D. Bates, S. DebRoy, D. Sarkar, & R Core Team (2020), *nlme: Linear and nonlinear mixed effects models. R package version 3.1-144*. Retrieved from https://CRAN.R-project.org/package=nlme>

Pirk, N., Santos, T., Gustafson, C., Johansson, A. J., Tufvesson, F., Parmentier, F. J., et al. (2015). Methane emission bursts from permafrost environments during autumn freeze-in: New insights from ground-penetrating radar. *Geophysical Research Letters*, *42*(16), 6732–6738. https://doi.org/10.1002/2015gl065034

Pirk, N., Tamstorf, M. P., Lund, M., Mastepanov, M., Pedersen, S. H., Mylius, M. R., et al. (2016). Snowpack fluxes of methane and carbon dioxide from high Arctic tundra. *Journal of Geophysical Research: Biogeosciences*, *121*(11), 2886–2900. https://doi.org/10.1002/2016JG003486

Polyakov, I. V., Beszczynska, A., Carmack, E. C., Dmitrenko, I. A., Fahrbach, E., Frolov, I. E., et al. (2005). One more step toward a warmer Arctic. *Geophysical Research Letters*, *32*(17), L17605. https://doi.org/10.1029/2005GL023740

R Core Team. (2018). R: A Language and Environment for Statistical Computing. Vienna: R Foundation for Statistical Computing.

Rains, F. A., P. C., Stoy, Welch, C. M., C., Montagne, & McGlynn, B. L. (2016). A comparison of methods reveals that enhanced diffusion helps explain cold-season soil CO_2 efflux in a lodgepole pine ecosystem. *Cold Regions Science and Technology*, *121*, 16–24. https://doi.org/10.1016/j.coldregions.2015.10.003

Raz-Yaseef, N., Torn, M. S., Wu, Y., Billesbach, D. P., Liljedahl, A. K., Kneafsey, T. J., et al. (2017). Large CO_2 and CH_4 emissions from polygonal tundra during spring thaw in northern Alaska. *Geophysical Research Letters*, *44*(1), 504–513. https://doi.org/10.1002/2016GL071220

Rivkina, E., Shcherbakova, V., Laurinavichius, K., Petrovskaya, L., Krivushin, K., Kraev, G., et al. (2007). Biogeochemistry of methane and methanogenic archaea in permafrost. *FEMS Microbiology Ecology*, *61*(1), 1–5. https://doi.org/10.1111/j.1574-6941.2007.00315.x

Roland, M., Vicca, S., Bahn, M., Ladreiter-Knauss, T., Schmitt, M., & Janssens, I. A. (2015). Importance of nondiffusive transport for soil CO_2 efflux in a temperate mountain grassland. *Journal of Geophysical Research: Biogeosciences*, *120*(3), 502–512. https://doi.org/10.1002/2014JG002788

Romanovsky, V. E., & Osterkamp, T. E. (2000). Effects of unfrozen water on heat and mass transport processes in the active layer and permafrost. *Permafrost and Periglacial Processes*, *11*(3), 219–239. https://doi.org/10.1002/1099-1530(200007/09)11:3<219:AID-PPP352>3.0.CO;2-7

Schuur, E. A. G., Bockheim, J., Canadell, J. G., Euskirchen, E., Field, C. B., Goryachkin, S. V., et al. (2008). Vulnerability of Permafrost Carbon to Climate Change: Implications for the global carbon cycle. *BioScience*, *58*(8), 701–714. https://doi.org/10.1641/B580807

Schuur, E. A., McGuire, A. D., Schädel, C., Grosse, G., Harden, J. W., Hayes, D. J., et al. (2015). Climate change and the permafrost carbon feedback. *Nature*, *520*(7546), 171–179. https://doi.org/10.1038/nature14338

Sellmann, P. V., & Brown, J. (1973). Stratigraphy and diagenesis of perennial frozen sediment in the Barrow, Alaska region. In *Permafrost: North American contribution to the Second International Conference* (pp. 171–181). Washington, DC: National Academy of Sciences.

Serreze, M. C., Bromwich, D. H., Clark, M. P., Etringer, A. J., Zhang, T., & Lawrence, R. (2002). Large-scale hydro-climatology of the terrestrial Arctic drainage system. *Journal of Geophysical Research*, *108*(D2), 8160–8188. https://doi.org/10.1029/2001JD000919

Shiklomanov, N. I., Streletskiy, D. A., Nelson, F. E., Hollister, R. D., Romanovsky, V. E., Tweedie, C. E., et al. (2010). Decadal variations of active-layer thickness in moisture-controlled landscapes, Barrow, Alaska. *Journal of Geophysical Research: Biogeosciences*, *115*(G4), G00I04. https://doi.org/10.1029/2009JG001248

Stähli, M., & Stadler, D. (1997). Measurement of water and solute dynamics in freezing soil columns with time domain reflectometry. *Journal of Hydrology*, *165*, 352–369. https://doi.org/10.1016/S0022-1694(96)03227-1

Sturtevant, C. S., Oechel, W. C., Zona, D., Kim, Y., & Emerson, C. E. (2012). Soil moisture control over autumn season methane flux, arctic coastal plain of Alaska. *Biogeosciences*, *9*(4), 1423–1440. https://doi.org/10.5194/bg-9-1423-2012

Subke, J. A., Heinemeyer, A., & Reichstein, M. (2009). Experimental design to scale up in time and space and its statistical considerations. In W. Kutsch, M. Bahn, & A. Heinemeyer (Eds.), *Soil carbon dynamics: An integrated methodology* (pp. 34–48). Cambridge, NY: Cambridge University Press.

Tagesson, T., Mölder, M., Mastepanov, M., Sigsgaard, C., Tamstorf, M. P., Lund, M., et al. (2012). Land-atmosphere exchange of methane from soil thawing to soil freezing in a high-Arctic wet tundra ecosystem. *Global Change Biology*, *18*(6), 1928–1940. https://doi.org/10.1111/j.1365-2486.2012.02647.x

Takagi, K., Nomura, M., Ashiya, D., Takahashi, H., Sasa, K., Fujinuma, Y., et al. (2005). Dynamic carbon dioxide exchange through snowpack by wind-driven mass transfer in a conifer-broadleaf mixed forest in northernmost Japan. *Global Biogeochemical Cycles*, *19*, GB2012. https://doi.org/10.1029/2004GB002272

Tang, J., Baldocchi, D. D., Qi, Y., & Xu, L. (2003). Assessing soil CO_2 efflux using continuous measurements of CO_2 profiles in soils with small solid-state sensors. *Agricultural and Forest Meteorology*, *118*, 207–220. https://doi.org/10.1016/S0168-1923(03)00112-6

Taş, N., Prestat, E., Wang, S., Wu, Y., Ulrich, C., Kneafsey, T., et al. (2018). Landscape topography structures the soil microbiome in arctic polygonal tundra. *Nature Communications*, *9*(1), 777. https://doi.org/10.1038/s41467-018-03089-z

Townsend-Small, A., Åkerström, F., Arp, C. D., & Hinkel KM, K. M. (2017). Spatial and temporal variation in methane concentrations, fluxes, and sources in lakes in Arctic Alaska. *Journal of Geophysical Research: Biogeosciences*, *122*(11), 2966–2981. https://doi.org/10.1002/2017JG004002

Treat, C. C., Bloom, A. A., & Marushchak, M. E. (2018). Nongrowing season methane emissions—a significant component of annual emissions across northern ecosystems. *Global Change Biology*, *24*(8), 3331–3343. https://doi.org/10.1111/gcb.14137

Wainwright, H. M., Dafflon, B., Smith, L. J., Hahn, M. S., Curtis, J. B., Wu, Y., et al. (2014). Identifying multiscale zonation and assessing the relative importance of polygon geomorphology on carbon fluxes in an Arctic tundra ecosystem. *Journal of Geophysical Research: Biogeosciences*, *120*(4), 788–808. https://doi.org/10.1002/2014JG002799

Wallenstein, M. D., McMahon, S. K., & Schimel JP, J. P. (2008). Seasonal variation in enzyme activities and temperature sensitivities in Arctic tundra soils. *Global Change Biology*, *15*(7), 1631–1639. https://doi.org/10.1111/j.1365-2486.2008.01819.x

Watanabe, K., & Ito, M. (2008). In situ observation of the distribution and activity of microorganisms in frozen soil. *Cold Regions Science and Technology*, *54*(1), 1–6. https://doi.org/10.1016/j.coldregions.2007.12.004

Webb, E. E., Schuur, E. A., Natali, S. M., Oken, K. L., Bracho, R., Krapek, J. P., et al. (2016). Increased wintertime CO_2 loss as a result of sustained tundra warming. *Journal of Geophysical Research: Biogeosciences*, *121*(2), 249–265. https://doi.org/10.1002/2014JG002795

Welker, J. M., Fahnestock, J. T., & Jones, M. H. (2000). Annual CO_2 flux in dry and moist arctic tundra: Field responses to increases in summer temperatures and winter snow depth. *Climate Change*, *44*, 139–150. https://doi.org/10.1023/A:1005555012742

Wilkman, E., Zona, D., Tang, Y., Gioli, B., Lipson, D. A., & Oechel, W. (2018). Temperature response of respiration across the heterogeneous landscape of the Alaskan Arctic tundra. *Journal of Geophysical Research: Biogeosciences*, *123*(7), 2287–2302. https://doi.org/10.1029/2017JG004227

Yanai, Y., Toyota, K., & Okazaki, M. (2004). Effect of a successive soil freeze-thaw treatment on soil microbial biomass and organic matter decomposition potential of soil. *Soil Science & Plant Nutrition*, *50*, 821–829. https://doi.org/10.1080/00380768.2004.10408542

Yu, X., Zou, Y., Jiang, M., Lu, X., & Wang, G. (2011). Response of soil constituents to freeze–thaw cycles in wetland soil solution. *Soil Biology and Biochemistry*, *43*(6), 1308–1320. https://doi.org/10.1016/j.soilbio.2011.03.002

Zhang, T., Frauenfeld, O. W., Ferenze, M. C., Etringer, A., Oelke, C., McCreight, J., et al. (2005). Spatial and temporal variability in active layer thickness over the Russian Arctic drainage basin. *Journal of Geophysical Research*, *110*, D16101. https://doi.org/10.1029/2004JD005642

Zimov, S. A., Davidov, S. P., Voropaev, V. Y., Prosiannikov, S., Semiletov, I. P., Chapin, M. C., & Chapin, F. S. (1996). Siberian CO_2 efflux in winter as a CO_2 source and cause of seasonality in atmospheric CO_2. *Climatic Change*, *33*, 111–120. https://doi.org/10.1007/BF00140516

Zimov, S. A., Semiletov, I. P., Daviodov, S. P., Voropaev, Y. V., Prosyannikov, S. F., Wong, C. S., & Chan, Y. H. (1993). Wintertime CO_2 emission from soils of northeastern Siberia. *Arctic*, *46*(3), 197–204.

Zimov, S. A., Zimova, G. M., Daviodov, S. P., Daviodova, A. I., Voropaev, Y. V., Voropaeva, Z. V., et al. (1993). Winter biotic activity and production of CO_2 in Siberian soils: a factor in the greenhouse effect. *Journal of Geophysical Research*, *98*, 5017–5023. https://doi.org/10.1029/92JD02473

Zona, D., Gioli, B., Commane, R., Lindaas, J., Wofsy, S. C., Miller, C. E., et al. (2016). Cold season emissions dominate the Arctic tundra methane budget. *Proceedings of the National Academy of Sciences*, *113*(1), 40–45. https://doi.org/10.1073/pnas.1516017113

Zona, D., Lipson, D. A., Zulueta, R. C., Oberbauer, S. F., & Oechel, W. C. (2011). Micro-topographic controls on ecosystem functioning in the Arctic Coastal Plain. *Journal of Geophysical Research*, *116*, G00I08. https://doi.org/10.1029/2009JG001241

Zona, D., Oechel, W. C., Kochendorfer, J., Paw U, K. T., Salyuk, A. N., Olivas, P. C., et al. (2009). Methane fluxes during the initiation of a large-scale water table manipulation experiment in the Alaskan Arctic tundra. *Global Biogeochemical Cycles*, *23*, GB2013. https://doi.org/10.1029/2009GB003487